HYDROGEN ABSTRACTION FROM *N*-BUTYL FORMATE BY H-RADICALS

W.A. Kopp* and K. Leonhard*
wassja.kopp@ltt.rwth-aachen.de
*Model-Based Fuel Design, Templergraben 55
RWTH Aachen University, 52062 Aachen, Germany

Abstract
Interest in the biofuel candidate *n*-butyl formate has increased due to new synthesis pathways and recently indicated negative temperature coefficient (NTC) behavior. Modeling is so far based on analogy estimates only and underlines the importance of initial hydrogen abstraction reactions. This study presents the (to our knowledge) first ab-initio reaction kinetics for *n*-butyl formate. Its numerous conformations are evaluated as well as their influence on reactions which facilitates further investigations. Hydrogen abstraction by H-Radicals is studied with the modern double hybrid density functional B2KPLYP that provides accurate barrier heights at feasible computational cost. Arrhenius expressions fitted in the temperature range from 800 K to 1200 K read for the lowest energy conformation:
abstraction from δ-carbon: $k(T) = 1.915 \times 10^{-18} \times T^{2.43} \exp(-33815\ \text{kJ/mol} / RT)$
abstraction from γ-carbon: $k(T) = 1.020 \times 10^{-18} \times T^{2.46} \exp(-23988\ \text{kJ/mol} / RT)$
abstraction from β-carbon: $k(T) = 1.501 \times 10^{-17} \times T^{2.13} \exp(-30467\ \text{kJ/mol} / RT)$
abstraction from α-carbon: $k(T) = 1.768 \times 10^{-18} \times T^{2.35} \exp(-26128\ \text{kJ/mol} / RT)$
abstraction from formate-carbon: $k(T) = 1.251 \times 10^{-18} \times T^{2.39} \exp(-28210\ \text{kJ/mol} / RT)$
Another low-energy conformation has been investigated but reaction rate differences to the lowest energy conformation have been found to be not significant.

Introduction
The main drawbacks of fossil fuels – their limited reserves and their release of before subterrestrially bound CO_2 – create interest in fuels derived from biomass [1]. In order to achieve a high overall efficiency of the whole energy supply process, the fuel production should take place at low temperatures and reduce the oxygen content of the biomass only partly since this requires additional energy. Furthermore, oxygen-containing fuels have the potential to reduce soot emissions in non-premixed combustion, so fuels derived from biomass often contain oxygen in different functional groups.

High-efficiency diesel and novel combustion concepts like Homogeneous Charge Compression Ignition (HCCI) use higher densities (and pressures) to increase efficiency while temperature is reduced (e.g. by exhaust gas recirculation) to avoid the formation of nitric oxides. The latter can also lead to a further increase of efficiency by reducing heat losses [2].
The negative temperature coefficient (NTC) behavior of fuels like diesel, *n*-heptane and DME [3] or *n*-butanol [4] improves ignitability at lower temperatures and so is an attractive fuel feature for high-efficiency low-temperature combustion concepts.

Recently measured ignition delay times of *n*-butyl formate at higher pressures and intermediate to low temperatures indicate that this fuel also shows NTC behavior [5]. Moreover, novel synthesis pathways for this fuel are under development that have the potential for new efficient production routes [6]. Butyl formate thus could be a promising new biofuel.

Despite this, the combustion chemistry of *n*-butyl formate has received little attention until very recently due to the lack of both experimental data and reaction rates for initiation steps. From the recently measured ignition delay times a chemical kinetic model has been derived that uses rates determined by analogy from similar species (ethanol, *n*-butanol, butane, methyl formate). The important initiation steps contain fuel decomposition and hydrogen abstraction reactions. The latter mainly take place by H, O, OH and HO_2 radicals. Calculating these reaction rates is difficult because of molecular size (increasing computational time) and because of the conformational complexity of butyl formate. This study therefore starts with an investigation of butyl formate conformations. So modeling can be focused on the most relevant structures. Based on that, hydrogen abstraction by H radicals is investigated.

Computational Methods

The gaussian program suite has been used throughout all of the calculations in the 03 and 09 versions [7]. Starting points for optimisation to local minimum conformations and transition state structures have been obtained from potential energy scans along the relevant dihedral angles or bond lengths. For all geometry optimisations and frequency calculations the B3LYP functional has been used with the tzvp basis set. Here DFT grid integration has been performed with an ultrafine grid and tight optimization convergence criteria have been applied. This functional is used because of its accurate frequencies that play an important role in thermochemistry. The standard deviation of frequencies from experiment is even lower than that of MP2 [8]. The frequencies should be obtained with the same method with which the geometry was obtained to do the frequency analysis in a minimum.

Modern fifth-rung density functionals include a second-order perturbation term (PT2) in addition to the hartree-fock (HF) exchange term in standard hybrid functionals [9] that makes them high-quality tools for equilibrium thermochemistry [10]. To make these functionals even better suited for kinetic purposes, special versions are available like the B2KPLYP functional where the two fractions of exchange for the HF and the PT2 part have been fitted to yield better barrier heights. In particular, for a set of 38 hydrogen transfer reactions, the B2KPLYP functional predicts barrier heights with a root mean squared error of 3.6 kJ/mol [11]. Therefore, based on the geometries obtained from B3LYP with tzvp basis set, single-point energies with the B2KPLYP functional have been computed. Since this version of the functional is not implemented in gaussian03, the mixing of the PT2 term and the rest has to be done manually by adding 0.42 times the E2 term to the SCF energy while these values are obtained as described in the original B2KPLYP paper [11] in footnote 47. Reaction rates have then been determined using conventional transition state theory (TST) together with tunneling along an eckart-shaped potential. This corresponds to the IVTST-0 option in polyrate2008 [12].

Conformations of Butyl Formate

A recent study on *n*-butanol reported 14 conformations of which 13 have a mirror image counterpart each [13]. We adopt the notation from there and compare our conformations with these results because of the similarity of *n*-butyl formate and *n*-butanol (only the terminal O-H is replaced by O-(C=O)-H). The additional group does not only introduce a further dihedral angle but also forbids some conformations allowed for *n*-butanol.

Figure 1: Molecular structure of *n*-butyl formate in its lowest energy conformation; nomenclature for the 4 dihedral angles relevant for conformer identification is shown. The angles are measured between heavy atoms.

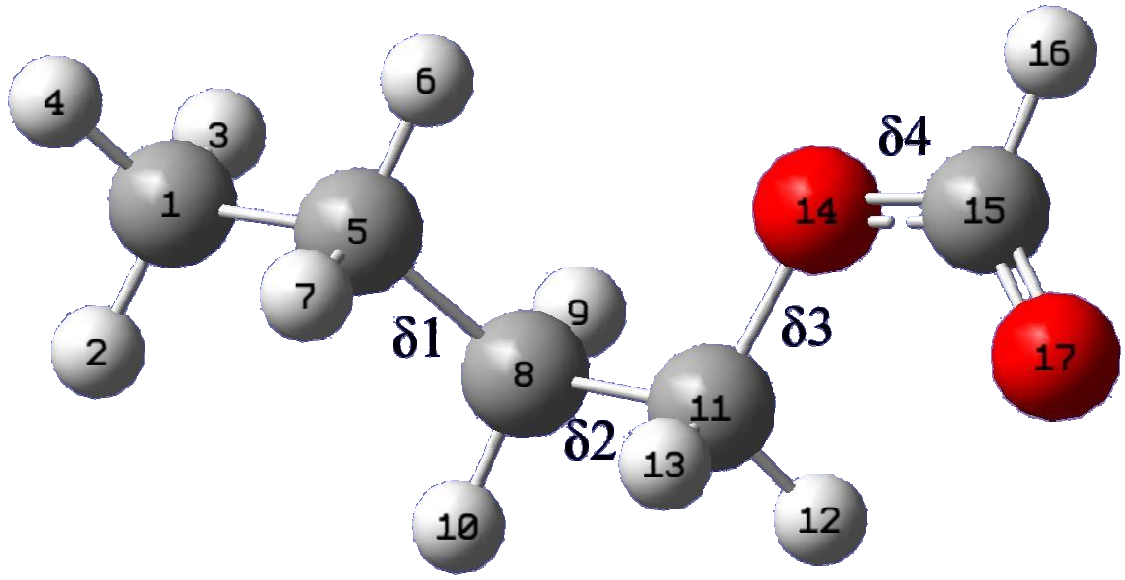

The notation is as follows (for the definition of the dihedral angles see figure 1): Dihedral angles near 180° are called *trans* and are abbreviated with t. Those near 0° (only δ4) are abbreviated with c like *cis* and the ones near 60° are called *gauche* and abbreviated with g or rather g' if they are near -60°. To use the analogy to *n*-butanol, in this study any angle between 30° and 150° is termed gauche. This extension only affects δ3 which is discussed below. According to figure 1, the conformations are thus termed δ1δ2δ3δ4 with the appropriate abbreviation inserted for δ*i*.

Table 1: Conformations of *n*-butyl formate with their 4 relevant dihedral angles and the corresponding energy on B3LYP/tzvp and B2KPLYP/aug-cc-pvtz level in kJ/mol. The last two columns contain the fraction of molecules in the respective conformation

Name	**δ1**	**δ2**	**δ3**	**δ4**	**B2K-PLYP**	**B3LYP**	**% (300K)**	**% (1000K)**
tg'tc	-179.1	-65.1	179.1	-0.1	0.0	0.0	27.98%	11.70%
tttc	180.0	180.0	180.0	0.0	0.6	0.4	13.64%	6.98%
ttgc	-179.6	176.2	87.6	0.3	1.1	1.7	13.84%	9.15%
tggc	179.5	61.5	88.7	0.2	1.7	2.2	10.92%	7.76%
g'g'tc	-64.7	-63.0	179.1	-0.1	2.3	3.0	10.06%	8.61%
gttc	65.9	176.9	179.1	0.1	3.7	3.9	6.94%	8.94%
gggc	64.2	58.7	88.2	0.3	3.9	5.0	4.02%	5.63%
gtgc	66.4	172.8	88.8	0.4	4.4	5.5	5.83%	6.39%
g'tgc	-66.2	178.9	87.8	0.4	4.6	5.5	3.34%	5.97%
g'gtc	-73.1	72.7	177.3	0.6	6.8	7.2	2.34%	6.54%

g'ggc	-70.9	70.4	88.6	0.0	7.6	8.7	0.93%	3.50%
tg'gt	-179.2	-65.9	128.7	178.9	18.9	18.6	0.04%	2.80%
tggt	180.0	61.5	107.6	-177.5	19.3	18.7	0.04%	3.01%
ttgt	-179.8	175.9	105.2	-177.6	19.8	19.0	0.04%	3.31%
gggt	64.3	58.5	104.1	-177.2	21.3	21.5	0.01%	1.88%
g'g'gt	-65.4	-63.8	137.7	177.8	21.3	21.8	0.02%	2.19%
gtgt	66.1	172.9	108.0	-178.0	22.9	22.6	0.01%	2.20%
g'tgt	-66.9	178.3	102.4	-177.3	23.2	22.8	0.01%	1.93%
gg'g't	73.0	-68.3	-107.6	177.8	25.3	25.1	0.00%	1.53%

Table 2: 14 reported conformations of *n*-butanol on B3LYP/6-311G(d,p) level [13], TGg', GGg' and GG'g have not been found for the *n*-butyl formate with δ4 in lower-energy *cis*-conformation

Name	**CC-CC[-OH]**	**[C-]CC-CO[-H]**	**[CC-]CC-OH**
TGt	-177.5	63.6	-176.2
TTt	180	180	180
TGg'	179.3	64.1	-70.4
TTg	179.3	176.5	61.3
GGg	66.9	57.0	61.8
GTg	66.5	174.0	62.1
G'Gt	-72.5	70.1	-179.2
TGg	-176.4	59.9	62.9
GTg'	66.5	-179.4	-59.6
GGg'	64.6	62.1	-69.9
GG'g	61.2	-79.7	68.6
GG'g'	71.5	-65.1	-59.2
GTt	66.0	176.7	178.2
GGt	66.2	60.6	-177.1

The additional functional group imposes changes on δ3 (C-C-O-C) compared to the *n*-butanol case (compare tables 1 and 2). The doubly bonded oxygen pulls electrons from the C15 carbon making it the only positively charged carbon of the molecule (compare figure 2 for the ttgc case). The more extended and positively charged formate C-H end thus feels more repulsion from the positive hydrogens of the other groups which it approaches to in the δ3-*gauche* conformations than the single -H end feels in *n*-butanol. This leads to an increased δ3 value of 88 ± 1° if δ4 is in *cis*-conformation (mainly the C15 is repelled) and even to 100° < δ3 < 130° if δ4 is in *trans*-conformation (C15 and H16 are repelled).

Furthermore, some conformations reported for *n*-butanol have not been found at all or only for one orientation of the O-(C=O)-H end. So the GG'g conformation is not favorable any more because the positive ends of the molecule approach each other like in a ring structure which is impossible here since both ends carry positive partial charges. Also the TGg' and the GGg' conformations appear only with the energetically much higher *trans*-position of δ4.

Figure 2: ttgc conformation with mulliken charges (B3LYP/tzvp), δ3=88°

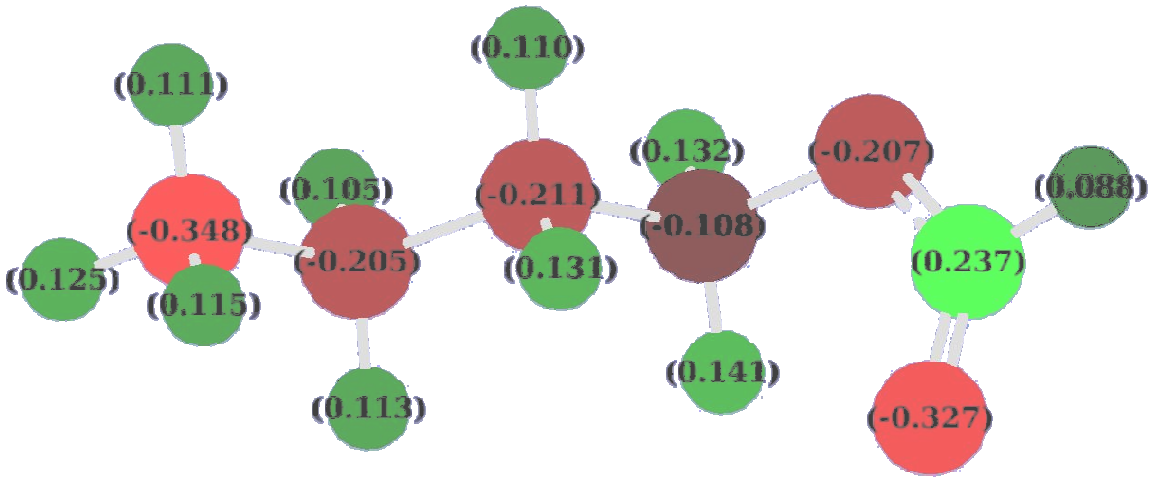

Energies of the conformations have been calculated on the B3LYP/tzvp level as a byproduct of the optimization as well as on the B2KPLYP/aug-cc-pvtz level since this has been used to determine the barrier heights for hydrogen abstraction by the H-radical. As can be seen in table 1, there is not much difference between the two methods. On the B2KPLYP level, the energies of conformations with lower relative energy (<9 kJ/mol) get even lower and separate further from the energies of conformations with higher energy (>18 kJ/mol) that remain approximately the same.

To determine the equilibrium distribution of conformations, the thermal correction to obtain gibbs free energy from the rigid-rotor harmonic-oscillator model has been added to the B2KPLYP energies. The conformations possessing a mirror image (all except tttc conformation) have been counted twice. From the diagram in figure 3 one can see that the 3 lowest energy conformations account for half of the *n*-butyl formate molecules at 300 K (approx. room temperature) and only for 28% of all molecules at 1000 K (which shall represent a “typical” temperature in ignition phenomena).

Figure 3: equilibrium distribution of *n*-butyl formate conformations based on B2KPLYP energies and B3LYP frequencies in the harmonic oscillator approximation according to table 1.
Inner ring: Distribution at 300 K
Outer ring: Distribution at 1000 K

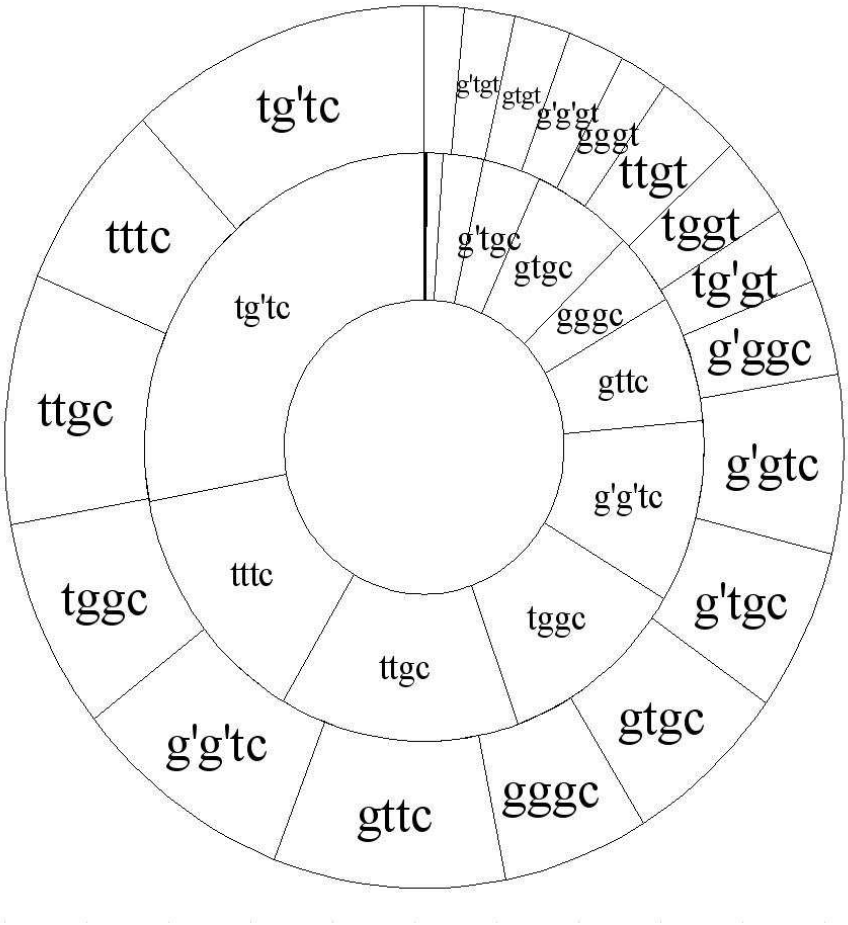

Since the lowest energy conformation constitutes only a minor part of the *n*-butyl formate molecules, it has to be clarified how these conformations affect reaction kinetics. To evaluate the influence of higher-energy conformations on kinetics, in addition to the lowest-energy tg'tc conformation also hydrogen abstractions from the higher tttc conformation have been studied and compared.

Barrier heights for hydrogen abstraction by H Radicals

In contrast to butyl formate, the reaction kinetics of methyl butanoate have been widely investigated. As a structural isomer of butyl formate, methyl butanoate, $CH_3(CH_2)_2(CO)OCH_3$ has the same molecular formula $C_5H_{10}O_2$. Its ignition behavior has been modeled extensively to use this fuel as a model for biodiesel [14]. Due to missing low temperature chemistry, methyl butanoate autoignition characteristics have turned out not to be similar to typical biodiesel behavior [15]. Barriers for hydrogen abstraction are reported in the literature on the BH&HLYP/cc-pVTZ level (see Table 3). The barriers are very low compared to unimolecular decomposition steps (e.g. 30 kJ/mol on average for H-radicals compared to 290 kJ/mol as lowest unimolecular decomposition height on BH&HLYP/cc-pVTZ level) [14]. The hydrogen abstraction reactions are therefore important initiation steps.

Table 3: Reported barrier heights for hydrogen abstraction reactions from methyl butanoate by H radicals at the BH&HLYP/cc-pvtz level in kJ/mol [14]

Product Radical	**H**
$CH_2°(CH_2)_2(CO)OCH_3$	34.7
$CH_3CH°CH_2(CO)OCH_3$	27.2
$CH_3CH_2CH°(CO)OCH_3$	25.1
$CH_3(CH_2)_2(CO)OCH_2°$	35.1

Since barriers for abstracting hydrogens of the same group can differ in energy and entropy, all 10 hydrogens of *n*-butyl formate have been investigated in this study. Characterstic data of these transition states are summarized in table 4.

Table 4: Characteristics of transition states of lowest *n*-butyl formate conformation + H with B3LYP geometries and frequencies and B2KPLYP energies.

hydrogen no.	Barrier [kJ/mol]	Reaction Energy [kJ/mol]	ν_{im} [i cm^{-1}]	H … H [Å]	C … H [Å]
2	50.72	2.12	1192	0.92663	1.36645
3	51.16	2.12	1199	0.92597	1.36653
4	52.18	3.42	1200	0.92341	1.36673
6	44.20	-9.21	1218	0.95346	1.32681
7	40.52	-9.21	1176	0.96536	1.31969
9	45.70	-4.64	1224	0.95088	1.33559
10	45.97	-4.64	1238	0.95720	1.33023
12	42.95	-11.79	1268	0.98961	1.29473
13	44.11	-11.79	1276	0.98464	1.30236
16	45.49	-12.61	1339	0.98935	1.31388

With decreasing distance from the formate group, the transition states become earlier and, corresponding to the Hammond postulate [16], the reaction energies are shifted into the exothermic direction, except for the C5 carbon group. Also the imaginary frequencies rise from 1200 to 1280 or even 1340 i cm^{-1} for H16, due to the larger curvature at the barrier. The barrier heights are ~50% larger than those reported for methyl butanoate that were obtained with a smaller basis set and an older hybrid functional.

To evaluate the influence of different conformations on reaction kinetics, we investigated the hydrogen abstraction also from the 2^{nd}-lowest conformation, the symmetric tttc conformation. The transition state chararcteristics are shown in table 5. The geometries differ from the other conformation only a few mÅ, the average difference in the barrier heights per group is shown in table 6. They differ from 0.6 to -1.2 kJ/mol while on average over all groups the barriers are 0.3 kJ/mol lower than for the lowest-energy conformation.

Table 5: Characteristics of transition states of 2nd-lowest *n*-butyl formate conformation (tttc) + H with B3LYP geometries and frequencies and B2KPLYP energies.

hydrogen no.	Barrier [kJ/mol]	Reaction Energy [kJ/mol]	ν_{im} [i cm^{-1}]	H … H [Å]	C … H [Å]
2, 3	51.54	2.60	1198	0.92515	1.36696
4	52.68	4.08	1200	0.92224	1.36833
6, 7	41.20	-9.66	1188	0.96540	1.31861
9, 10	44.97	-3.88	1213	0.95150	1.33224
12, 13	43.02	-11.88	1265	0.98731	1.29790
16	45.72	-12.25	1340	0.98842	1.31462

Table 6: Difference of hydrogen abstraction barrier heights averaged per group from 2nd lowest to lowest energy conformation

Hydrogens	Conf.2 – Conf.1
2,3,4	0.57
6,7	-1.16
9,10	-0.86
12,13	-0.51
16	0.24
average:	-0.31

In the next section it will be shown how this affects the reaction rates.

Reaction Rates

Reaction Rates for hydrogen abstraction by hydrogen radicals have not been found in the literature and are computed based on the transition state information (B2KPLYP energies) presented above. Arrhenius expressions for the rates of abstraction from the lowest energy conformation read for

abstraction from C1: $k(T) = 1.915 \times 10^{-18} \times T^{2.43} \exp(-33815\ \text{kJ/mol} / RT)$

abstraction from C5: $k(T) = 1.020 \times 10^{-18} \times T^{2.46} \exp(-23988\ \text{kJ/mol} / RT)$

abstraction from C8: $k(T) = 1.501 \times 10^{-17} \times T^{2.13} \exp(-30467\ \text{kJ/mol} / RT)$

abstraction from C11: $k(T) = 1.768 \times 10^{-18} \times T^{2.35} \exp(-26128\ \text{kJ/mol} / RT)$

abstraction from C15: $k(T) = 1.251 \times 10^{-18} \times T^{2.39} \exp(-28210\ \text{kJ/mol} / RT)$

These expressions have been fitted from 800 K to 1200 K to the data presented in figure 4, units are molecule, second and cm^3.

Figure 4: Arrhenius plot of reaction rates obtained by IVTST-0 method for hydrogen abstraction from the different carbon atoms (according to figure 1) in lowest energy tg'tc conformation by H-Radicals. Units are molecule, second and cm³.

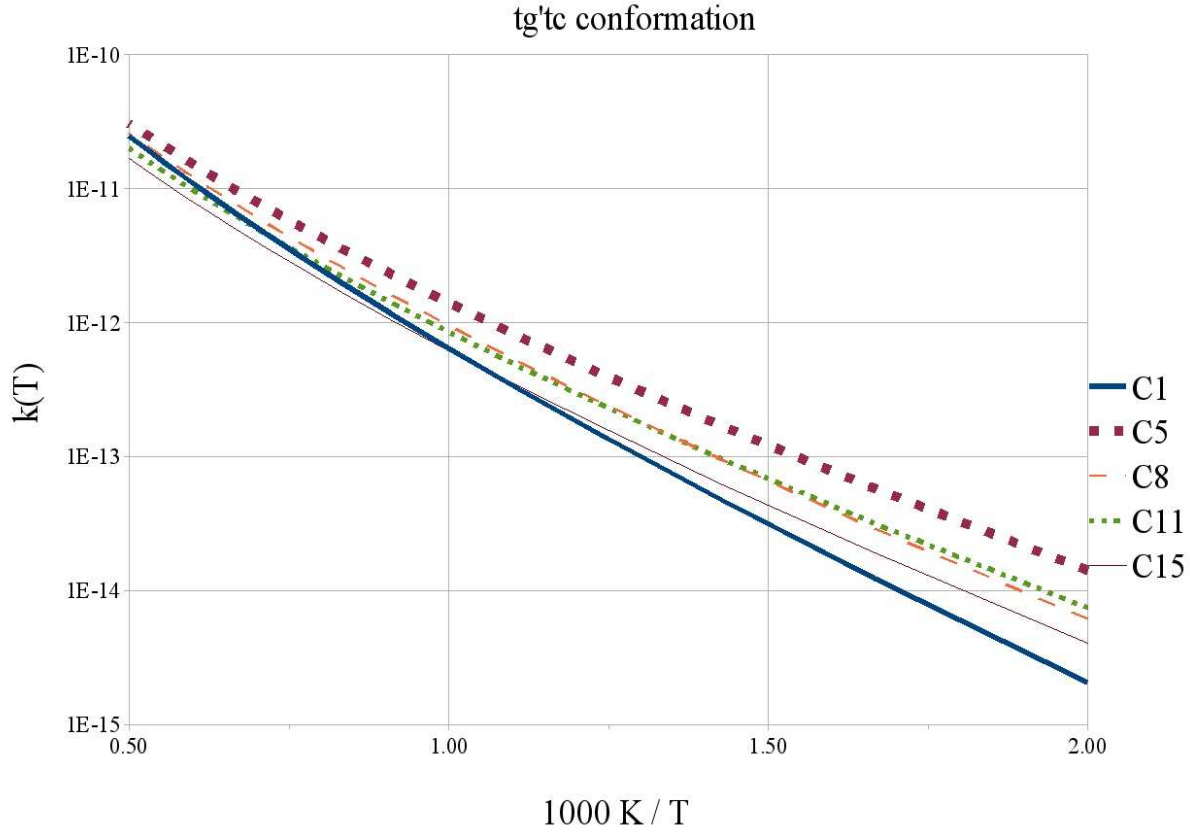

To check how reaction kinetics change treating another conformation, we ran the IVTST-0 calculations also for the tttc conformation. Here again Arrhenius expressions have been fitted from 800 to 1200 K, for

abstraction from C1: $k(T) = 4.532 \times 10^{-18} \times T^{2.34} \exp(-35234 \text{ kJ/mol} / RT)$
abstraction from C5: $k(T) = 2.698 \times 10^{-18} \times T^{2.34} \exp(-24086 \text{ kJ/mol} / RT)$
abstraction from C8: $k(T) = 4.559 \times 10^{-18} \times T^{2.27} \exp(-28307 \text{ kJ/mol} / RT)$
abstraction from C11: $k(T) = 6.379 \times 10^{-18} \times T^{2.19} \exp(-26965 \text{ kJ/mol} / RT)$
abstraction from C15: $k(T) = 1.108 \times 10^{-18} \times T^{2.41} \exp(-28190 \text{ kJ/mol} / RT)$

to the data shown in figure 5.

Figure 5: Same as figure 4, but for the 2nd lowest energy tttc conformation.

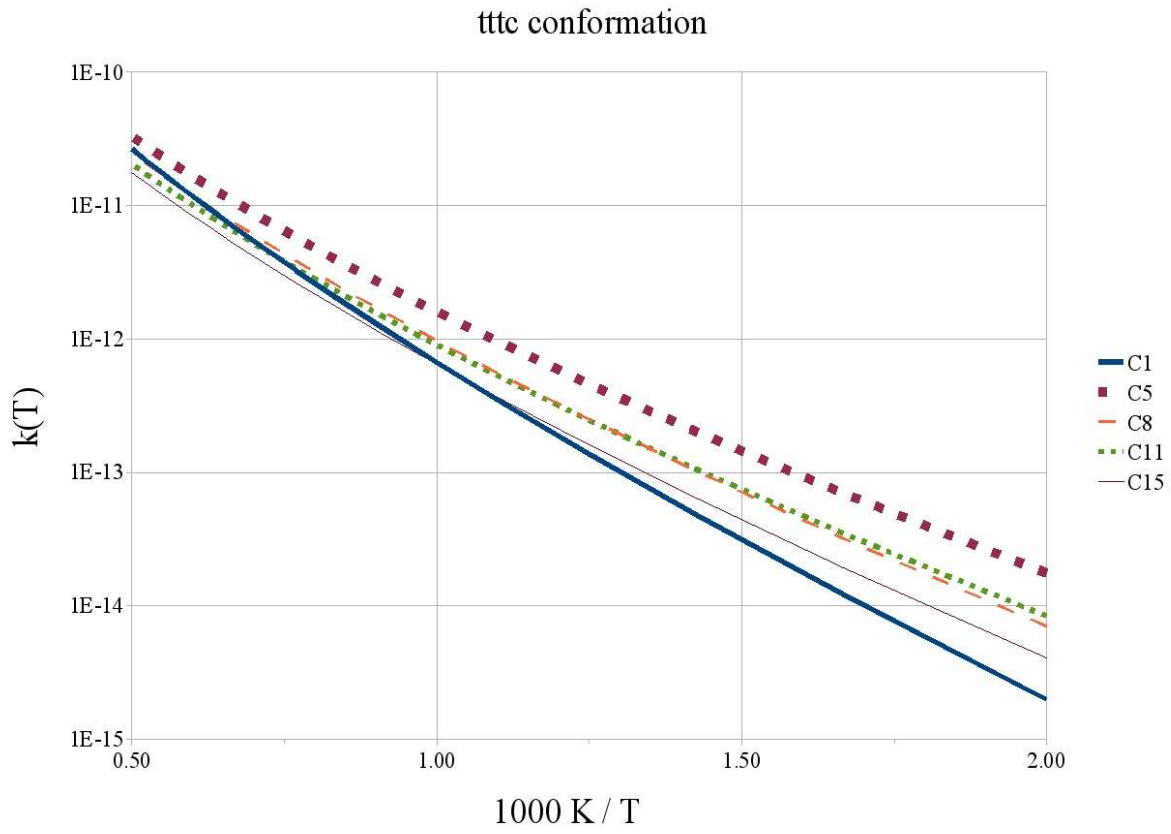

The results show that reaction kinetics are influenced only little by the different geometries, energies and frequencies of the conformations. The ratio of the elementary reaction rates for abstraction from the two conformations range from 0.9 to 1.3 except for abstraction from H6 at lower temperatures where the ratio amounts to 1.8 at 500 K but falls with increasing temperature.

The small influence of different conformations on the reaction rates may change with increasing complexity of the radical reactant since there will be more possibilities to interact with the rest of the molecule in a particular conformation. This may also be seen in the important reactions with OH and HO_2 radicals which are our next targets.

Conclusion

In this work, the numerous conformations of *n*-butyl formate have been examined and compared to already investigated compounds (*n*-butanol). Reaction rates for abstraction from the two lowest energy conformations have been presented. The difference between kinetics for the two conformations is small which may be different for more complicated radicals and shall be subject to further studies. The presented rates will hopefully contribute to improved future mechanisms for the promising biofuel candidate butyl formate.

This work was performed as part of the Cluster of Excellence "Tailor-Made Fuels from Biomass", which is funded by the Excellence Initiative by the German federal and state governments to promote science and research at German universities.

References

[2] Manley, D.K., McIlroy, A., Taatjes, C.A., "Research needs for future internal combustion engines", *Physics Today* 61, 11, pp. 47–52 (2008)

[3] Pfahl, U., Fieweger, K., Adomeit, G., "Self-ignition of diesel-relevant hydrocarbon-air mixtures under engine conditions", *26th Symp. Int. Comb.* 1&2, 781–789 (1996)

[4] Vranckx, S., Heufer, K.A., Lee, C., Olivier, H., Schill, L. , Kopp, W.A., Leonhard, K., Taatjes, C.A., Fernandes, R.X., "Role of peroxy chemistry in the high pressure ignition of *n*-butanol – Experiments and detailed kinetic modelling", *Comb. Flame*, DOI: 10.1016/j.combustflame.2010.12.028 (2011)

[5] Lee, C., Vranckx, S., Fernandes, R.X., "Low and inter-mediate temperature oxidation of butyl formate at elevated pressures", *Proc. Europ. Comb*., in press (2011)

[6] Klankermayer, J., *et al.*, personal communication 2011

[7] Frisch, M.T., *et al*., Gaussian03, version e.01 and Gaussian09, version a.01, Gaussian Inc., Wallingford CT, 2004

[8] Irikura, K.K, Johnson III, R.D, Kacker, R.N., "Uncertainties in Scaling Factors for ab Initio Vibrational Frequencies", *J. Phys. Chem. A*, 109, 8430-8437 (2005)

[1] Kohse-Höinghaus, K., Osswald, P., Cool, T.A., Kasper, T., Hansen, N., Qi, F., Westbrook, C.K., Westmoreland, P.R., *Angew. Chem., Int. Ed.* 49 (2010) 3572–3597.

[9] S. Grimme, *J. Chem. Phys.* 124, 34108 (2006)

[10] Raghavachari, K.; Curtiss, L. A. In "Quantum-Mechanical Prediction of Thermochemical Data"; Cioslowski, J., Ed.; Kluwer: Dordrecht, The Netherlands, 2001; pp 67–98.

[11] Tarnopolsky, A., Karton, A., Sertchook, R., Vuzman, D., Martin, J.M.L., "Double-Hybrid Functionals for Thermochemical Kinetics", *J. Phys. Chem. A* 112, 3–8 (2008)

[12] Zheng, J., *et al*., POLYRATE, 2008.

[13] Moc, J., Simmie, J.M., Curran, H.J., "The elimination of water from a conformationally complex alcohol: A computational study of the gas phase dehydration of *n*-butanol", *J. Mol. Struct.* 928: 149-157 (2009)

[14] Huynh, L.K., Lin, K.C., Violi, A., "Kinetic Modeling of Methyl Butanoate in Shock Tube", *J. Phys. Chem. A* 112: 13470-13480 (2008)

[15] Gail, S., Thomson, M.J., Sarathy, S.J., Syed, S.A., Dagaut, P., Dievart, P., Marchese, A.J., Dryer, F.L., "A wide-ranging kinetic modeling study of methyl butanoate combustion", *Proc. Comb. Inst.* 31: 305-311 (2007)

[16] Hammond, G.S., "A Correlation of Reaction Rates". *J. Am. Chem. Soc.* 77, 334–338 (1955)